Dual-Mode Light Transduction through a Plastically Bendable Organic Crystal as Optical Waveguide

Luca Catalano,[†] Durga Prasad Karothu,[†] Stefan Schramm,[†] Ejaz Ahmed,[†] Rachid Rezgui,[†] Timothy J. Barber,[†] Antonino Famulari[I] and Panče Naumov*[†]

[†]New York University Abu Dhabi, P.O. Box 129188, Abu Dhabi, United Arab Emirates

[I]Politecnico di Milano, Piazza Leonardo Da Vinci 32, 20133 Milano, Italy

Supporting Information Placeholder

ABSTRACT: An anthracene derivative, 9,10-dicyanoanthracene, crystallizes as fluorescent acicular single crystals that can be readily plastically bent in two directions. Spatially resolved photoluminescence analysis revealed that this material is endowed with robust optoelectronic properties that are preserved upon extreme crystal deformation. The highly flexible crystals were successfully tested as efficient switchable optical waveguiding elements for both active and passive light transduction, the mode of operation depending on the wavelength of the incident light. This prototypical dual-mode organic optical crystalline fiber brings mechanically compliant molecular organic crystals closer to applications as novel light-transducing media for wirelessly direct functional response in all-organic microoptoelectronic devices.

Unlike electron conductivity through metal conductors, transduction of light is inherently impervious to interference with external electromagnetic fields, and this calls for new organic materials as light-weight, cost-effective and secure optical transducers of information. The favorable optical properties and long-range order of molecular crystals is increasingly being recognized as a new platform for advancement of metal-free, all-organic electronics and soft robotics. Poor processing ability and less-than-optimal mechanical properties of the organic crystals, and particularly their pronounced brittleness and fragility, however, are usually taken as major impediments against their implementation in flexible devices, where thin organic films have long been superior and preferred phase of choice. The recent advent of methodologies for controlled crystal growth has provided strategies for fairly good control over the habit, the aspect ratio and mosaic spread of molecular crystals.[1] Moreover, the burgeoning research into mechanical properties or molecular crystals has revealed that certain organic crystals can be extraordinarily mechanically compliant; they are endowed with extraordinary mechanical properties such as elasticity and plasticity that is comparable to those of metallic conductors.[2] By having a solution to these two major drawbacks overcome, the molecular crystals now evolve as material of choice for all-organic electronics,[3] soft robotics,[4] smart materials[5] and optoelectronics.[6] Along this line of pursuit, recent reports have described organic crystals as optical waveguides for implementation in integrated optical nano/microcircuits,[7] although these studies are limited to a few examples of elastically bendable crystals.[8] Depending on the nature of the propagated light, organic crystalline waveguides are classified as active or passive.[9] Active waveguides are generally based on luminescent π-conjugated species having electronic absorption windows in the UV-visible region that are able to propagate their photoluminescence emission at the extremities of the crystals.[9,10] Passive organic waveguides, on the other hand, propagate the input light unaltered to the output end. Here we report a fluorescent organic crystal, 9,10-dicyanoanthracene (DCA), that can be used as optical waveguide and bent plastically to acute angles without fracture. We establish that this material can transduce light both by transmission and emission, and the mode of light transduction can be switched by changing the excitation wavelength. This mechanically compliant single crystal sets the path to future application of similar organic crystals as dual-mode light waveguides.

When crystallized by slow evaporation from a variety of organic solvents (toluene, nitrotoluene, nitrobenzene and chlorobenzene), DCA consistently affords long yellow crystals that are 50–300 μm thick and up to about 1 cm long, together with a small fraction of parallelepiped blocks. Similar to the structure at 100 K,[11] the structure of the crystals at room temperature, which is identical for both crystal habits, is triclinic (space group $P\bar{1}$), with a single molecule per unit cell (details on the structure analysis are available from the Supporting Information, SI).

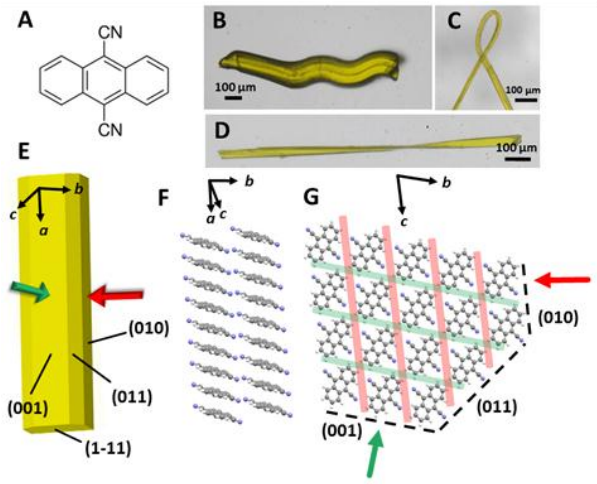

Figure 1. Mechanical properties and structure of optically transducing crystal, 9,10-dicyanoanthracene (DCA). (A) Chemical structure. (B–D) Examples of plastic deformation of crystals, shown here as multiple bending (B), bending over 180° (C), and twisting (D). (E) Schematic of a typical habit of DCA crystal with face indices. The two faces on which the crystal is plastically bendable are highlighted with arrows: (001) (green arrow) and (010) (red arrow). (F) Columnar π—π stacking along the crystallographic *a* axis. (G) Crystal structure of DCA viewed in the [100] direction. The slip planes responsible for the 2D plasticity are parallel to the (001) (green arrow) and (010) (red arrow) faces.

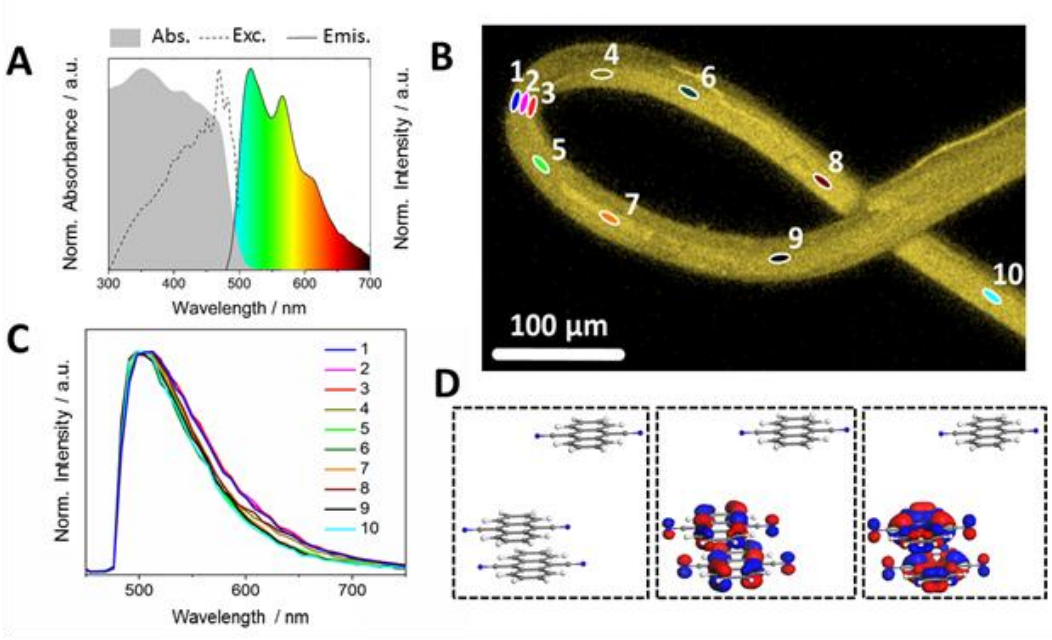

Figure 2. Photophysical properties of DCA. (A) Absorption, excitation and emissions spectra of DCA recorded from powder samples. (B) Confocal fluorescence microscopy image of highly bent DCA crystal. Locations labeled 1–10 (spot area = 36.88 µm^2) were selected to calculate the local average emission spectra across the crystal. (C) Average spectral emission spectra extracted from the locations 1–10 in panel B. The spectra are nearly identical, and confirm that the emission does not depend significantly on the bending of the crystal. (D) From left to right, a representative distorted trimer and the relative frontier orbitals involved in the main emission band, which after separation of one molecule from the trimer remain localized on the molecules of the π-stacked dimer.

Inspection of the molecular arrangement and intermolecular interactions indicates that the central structural feature responsible for their plasticity are the strong π—π interactions between the anthracene cores that are stacked in parallel offset fashion. The DCA molecules are arranged in columns in the [100] direction, with interplanar distance between the molecules of 3.46 Å and centroid-to-centroid distance of 3.89 Å (Figure 1F, SI Figure S1). DFT calculations (SI) confirmed that the π—π interactions are the main driving force for the molecular self-assembly, with interaction energy between the adjacent molecules of ~32 kcal/mol.

As shown in Figure 1B–D, the crystals are remarkably plastic; they can be manually bent to an arbitrary shape by applying pressure at a single point or at multiple locations in any direction perpendicular to their long axis. By careful manual micromanipulation, the crystals can be twisted (Figure 1D), and bent acutely (Figure 1C). Face indexing (Figure 1E and SI Figure S2) revealed that the crystals bend plastically when they are subjected to force perpendicular to their (001) and (010) faces (Figures 1E and 1G). As with other similar π-conjugated systems,[2e,12] the 2D plasticity of DCA crystals can be attributed to presence of dispersive interactions between π-stacked columnar assemblies of molecules.[13] Weak (van der Waals) interactions comprise smooth slip planes, (001) and (010), and facilitate slippage of the adjacent DCA columns, ultimately resulting in pronounced plasticity in two dimensions (Figure 1G). The weak interacting nature of these planes was confirmed by energy framework calculations, which returned interaction energies ranging from 1.5 to 5.7 kcal/mol for (001) plane and from 1.5 to 4.1 kcal/mol for (010) plane (further details are provided in the SI section 6).[14] The Young's modulus (E), measured by three-point flexural test on the (001) face, the widest facet of the needle-like crystals, averaged over four samples is E = 0.6 ± 0.2 GPa. This value is comparable to other flexible organic crystals[3a] and is consistent with their pronounced softness (further details are available from the SI and SI Movie 1).

Having the structural basis for plasticity of the crystals clarified, we focused on their photophysical characterization to assess the effect of deformation on the optoelectronic properties. DCA powders show bright green/yellow fluorescence with a maximum at 516 nm with vibronic peaks at 565 nm and 610 nm, emission lifetime τ = 12.0 ± 0.1 ns, and internal quantum yield Φ_{int} = 7.4%. The absorbance and emission spectra overlap in the 480–550 nm range (Figure 2A; see SI for further details). Compared to the solution spectra, organization of the molecules in the crystal results in remarkable bathochromic shifts (~100 nm) in both absorption and fluorescence. The shifts are due to formation of J-aggregates, which lower the energy band gap of DCA (Figure 1A and SI Figure S3).[11,15] The J-aggregates are known to be extremely sensitive to their relative arrangement in the crystal, and it is anticipated that even minor structural perturbations will result in shifts of the emission that are generally detectable with naked eye.[16]

To assess the eventual effect of bending on the emission, a representative acutely deformed single crystal of DCA was examined by using confocal fluorescence microscopy (Figure 2B and 2C). The average emission was recorded from ten sample locations of fixed area across the crystal. Apart from the apparent minor red-shift due to partial reabsorption of light, no other appreciable changes could be detected between the straight and bent sections. Furthermore, the fluorescence lifetime is uniform across the crystal, and provides evidence of identical radiative pathway of the molecules in the straight and distorted sectors (Figure S5). To rationalize these observations, the emission spectra were calculated by time-dependent DFT calculations on DCA monomers, dimers and trimers that were extracted from the crystal structure (SI).[17] The optimized trimers reproduced well the fluorescence of the bulk crystal. To simulate the atomic-level structural deformation and its effect on the optoelectronic properties, columnar trimers were distorted in different geometries and their emission spectra were calculated (SI). It was hypothesized that the invariant emission of highly distorted DCA crystals is rooted in two concomitant effects,

the strong π—π interactions between the first-neighbor molecules and the localization of molecular orbitals. Disruption of the trimer by shifting one molecule far from the optimized columnar assembly resulted in localization of the frontier molecular orbitals that contribute to the main emission band (calculated at 485 nm) on the remaining undistorted π-stacked dimer. This did not affect significantly the emission maximum (xx nm) and preserved the strong molecular orbital overlap (Figure 2D and SI section 6) confirming that the emission comes from the dimers which are not significantly perturbed during bending.

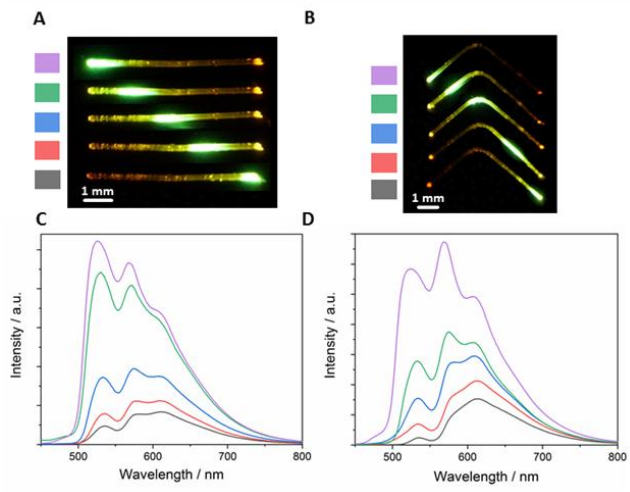

Figure 3. Light transduction by straight and bent DCA crystals excited with a 365 nm LED light. (A,B) Dark-field photographs of fluorescence from straight (A) and bent (B) crystals. (C,D) Fluorescent spectra recorded at the end of the straight (C) and bent (D) crystals by changing the distance between the point of excitation and the end of the crystal. The spectra are color-coded with the respective colors of the squares in panels A and B.

The retention of the optoelectronic properties upon mechanical deformation favors DCA crystals as flexible active optical waveguides. When excited with 365 nm light at one end, rod-like crystals transmit light to the opposite end (see section 3 in the SI and SI Figure S6). The color of the incident light is visibly changed from yellow-green to orange due to partial reabsorption by the crystal. The waveguide capabilities were investigated on both straight and bent samples. Figure 3 shows emission collected at one end of a crystal upon localized excitation with a 365 nm CW LED perpendicular to the long axis and at different positions (for details, see section 5 in the SI). The emission intensity at the tip of the crystal (I_{tip}) decreases gradually from the intensity at the point of excitation (I_{body}) along the crystal with increasing distance between the tip and the excitation point. The optical waveguiding efficiency was calculated following a previously reported procedure (SI Figure S7),[7] by single-exponential fit of the spectra in Figure 3 with the equation $I_{tip}/I_{body} = \exp(-\alpha D)$, where α (in mm^{-1}) is the optical loss coefficient of the crystals and D is defined as the distance between the tip and the excitation point. For a 7.4 mm long straight crystal, at 530, 570 and 610 nm, α', which is the optical loss conveniently expressed in dB mm^{-1} ($\alpha' \approx 4.34\,\alpha$; see SI for details), was estimated to be 1.6 ± 0.3, 1.2 ± 0.1 and 0.9 ± 0.2 dB mm^{-1} respectively. These values are in line with recently reported crystalline optical waveguides based on small molecules with optical loss, α' (1–3 dB mm^{-1}), and favors DCA as a suitable candidate for construction of integrated optical microcircuits.[7k–l,8,18] The decrease of α' from 530 to 610 nm is due to reabsorption of the crystal below 550 nm, which also results in change in the relative emission intensities of the vibronic peaks and their apparent red-shift. Similar optical performance was obtained for a 7.8 mm bent crystal, with respective values of α' at 530, 570 and 610 nm of 1.9 ± 0.2, 1.35 ± 0.04, and 0.65 ± 0.09 dB mm^{-1}, and highlight the robust optoelectronic properties of the DCA crystals.

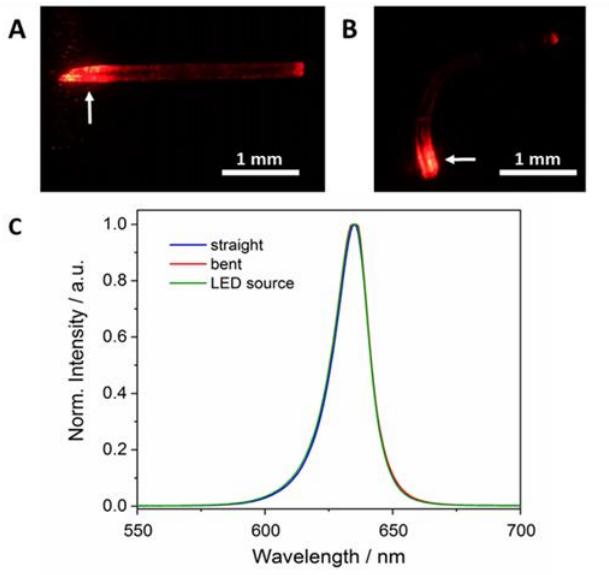

Figure 4. Transduction of red light by a straight and subsequently bent DCA crystal. (A,B) Dark-field photographs showing the transduction of 625 nm light by the crystal before (A) and after bending (B). The white arrows indicate the light input. (C) Normalized spectra of the input LED source and the output light from the crystal before and after bending, showing the passive waveguiding properties of the crystal.

The combination of active and passive functionality in a single organic optical waveguide, which has recently been established as one of the open challenges in this research direction,refs is accomplished with DCA by taking advantage of its high refractive index and solid-state photophysics.[9] The absorption window of crystalline DCA closes above 550 nm, and is in line with the lowering of α' on going from 530 nm to 610 nm, given that the optical loss coefficient is the sum of two main contribution, namely absorption and light scattering due to defects and surface roughness.[7k] Thus, we used a red CW LED (nominal emission wavelength, 625 nm; actual wavelength: 635 nm) as input signal in a 3.3 mm DCA crystal as waveguide in both straight and bent states to check the passive waveguiding properties of the prototypical fiber (Figure 4). As expected, the source light was transported through both straight and bent crystal with unaltered normalized spectrum, confirming the ability for passive (in addition to active) transduction of light by the DCA crystals (Figure 4C). The passive waveguiding efficiency is only limited by the presence of defects in the crystal lattice.

In summary, plastically bendable crystals of commercially available anthracene derivative that can be bent on two faces were prepared, and their use as hybrid active-passive optical waveguides was explored. The structural origin of the plasticity is assigned to orthogonal weak dispersive forces and π—π interactions. These fluorescent soft organic crystals were successfully tested as both active and passive optical waveguides, and exhibited optical loss coefficients that are comparable to the most efficient molecular crystalline waveguides reported to date. The optoelectronic properties are preserved upon extreme mechanical deformation. Furthermore, by taking advantage of the solid-state photophysics of the material, it was possible to demonstrate switching between the active and the passive waveguiding functionalities simply by changing the input light source. The results presented here favor these and other mechanically compliant organic crystals as promising candidates for construction of future low-cost flexible smart optoelectronic devices with advantageous mechanical properties.

ASSOCIATED CONTENT

Supporting Information

The Supporting Information is available free of charge on the ACS Publications website. Materials, methods, experimental techniques, supplementary figures and tables (PDF). Three-point flexural test (AVI)

AUTHOR INFORMATION

Corresponding Author

pance.naumov@nyu.edu

ACKNOWLEDGMENT

We thank New York University Abu Dhabi for financial support. A.F. acknowledge MURST (PRIN: 2015XJA9NT_003) and CINECA.

REFERENCES AND NOTES

(1) Lovette, M. A.; Browning, A. R.; Griffin, D. W.; Sizemore, J. P.; Snyder, R. C.; Doherty, M. *Ind. Eng. Chem. Res.* **2008**, *47*, 9812-9833.

(2) (a) Reddy, C. M.; Padmanabhan, K. A.; Desiraju, G. R. *Cryst. Growth Des.* **2006**, *6*, 2720-2731; (b) Takamizawa, S.; Miyamoto, Y. *Angew. Chem. Int. Ed.* **2014**, *53*, 6970-6973; (c) Naumov, P.; Chizhik, S; Panda, M. K.; Nath, N. K.; Boldyreva, E. *Chem. Rev.* **2015**, *115*, 12440-12490; (d) Panda, M. P.; Ghosh, S.; Yasuda, N.; Moriwaki, T.; Mukherjee, G. D.; Reddy, C. M.; Naumov, P. *Nat. Chem.*, **2015**, *7*, 65-72; (e) Krishna, G. R.; Devarapalli, R.; Lal, G.; Reddy, C. M. *J. Am. Chem. Soc.* **2016**, *138*, 13561-13567; (f) Pejov, L.; Panda, M. K.; Moriwaki, T.; Naumov, P. *J. Am. Chem. Soc.*, **2017**, *139*, 2318-2328; (g) Thomas, S. P.; Shi, M. W.; Koutsantonis, G. A.; Jayatilaka, D.; Edwards, A. J.; Spackman, M. A. *Angew. Chem. Int. Ed.* **2017**, *56*, 8468-8472; (h) Mir, S. H.; Takasaki, Y.; Engel, E. R.; Takamizawa, S. *Angew. Chem. Int. Ed.*, **2017**, *56*, 15882-15885; (i) Worthy, A.; Grosjean, A.; Pfrunder, M. C.; Xu, Y.; Yan, C.; Edwards, G.; Clegg, J. K.; McMutrie, J. C. *Nat. Chem.*, **2018**, *10*, 65-69.

(3) (a) Owczarek, M.; Hujsak, K. A.; Ferris, D. P.; Prokofjevs, A.; Majerz, I.; Szklarz, P.; Zhang, H.; Sarjeant, A. A.; Stern, C.L.; Jakubas, R.; Hong, S.; Dravid, V. P.; Stoddart, J. F. *Nat. Commun.* **2016**, *7*, 13108; (b) Kazantsev, M. S.; Kostantinov, V. G.; Dominiskiy, I. D.; Bruevich, V. V.; Postnikov, V. A.; Luponosov, Y. N.; Tafeenko, V. A.; Surin, N. M.; Ponomarenko, S. A.; Parashuk, D. Y. *Synth. Met.* **2017**, *232*.

(4) (a) Commins, P.; Hara, H.; Naumov, P. *Angew. Chem. Int. Ed.* **2016**, *55*, 13028-13032; (b) Taniguchi, T.; Sugiyama, H.; Uekusa, H.; Shiro, M.; Asahi, T.; Koshima, H. *Nat. Commun.* **2018**, *9*, 538.

(5) Gupta, P.; Karothu, D. P.; Ahmed, E.; Naumov, P.; Nath, N. K. *Angew. Chem. Int. Ed.* **2018**, *57*, 8498-8502.

(6) (a) Krishna, G. R.; Kiran, M. S. R. N.; Fraser, C. L.; Ramamurty, U.; Reddy, C. M. *Adv. Funct. Mater.* **2013**, *23*, 1422-1430; (b) Hayashi, S.; Koizumi, T. *Angew. Chem. Int. Ed.* **2016**, *55*, 2701-2704.

(7) (a) Yanagi, H.; Morikawa, T. *Appl. Phys. Lett.* **1999**, *75*, 187-189; (b) Yanagi, H.; Ohara, T.; Morikawa, T. *Adv. Mater.* **2001**, *13*, 1452-1455; (c) Ichikawa, M.; Hibino, R.; Inoue, M.; Haritani, T.; Hotta, S.; Koyama, T.; Taniguchi, Y. *Adv. Mater.* **2003**, *15*, 213-217; (d) Balzer, F.; Bordo, V. G.; Simonsen, A. C.; Rubahn, H.-G. *Phys. Rev. B* **2003**, *67*, 115408; (e) Quochi, F.; Cordella, F.; Mura, A.; Bongiovanni, G.; Balzer, F.; Rubahn, H.-G. *Appl. Phys. Lett.* **2006**, *88*, 041106; (f) Bao, Q.; Goh, B. M.; Yan, B.; Yu, T.; Shen, Z.; Loh, K. P. *Adv. Mater.* **2010**, *22*, 3661, 3666; (h) Zhang, C.; Zhao, Y. S.; Yao, J. *Phys. Chem. Chem. Phys.* **2011**, *13*, 9060-9073; (h) Chandrasekhar, N.; Chandrasekar, R. *Angew. Chem. Int. Ed.* **2012**, *51*, 3556-3561; (i) Yao, W.; Yan, Y.; Xue, L.; Zhang, C.; Li, G.; Zheng, Q.; Zhao, Y. S.; Jiang, H.; Yao, J. *Angew. Chem. Int. Ed.* **2013**, *52*, 8713-8717; (j) Zhu, W.; Zheng, R.; Zhen, Y.; Yu, Z.; Dong, H.; Fu, H.; Shi, Q; Hu, W. *J. Am. Chem. Soc.* **2015**, *137*, 11038-11046; (k) Chen, J.; Ma, S.; Zhang, J.; Li, B.; Xu, B.; Tian, W. *ACS Photonics* **2015**, *2*, 313-318; (l) Li, Y.; Ma, Z.; Li, A.; Xu, W.; Wang, Y.; Jiang, H.; Wang, K.; Zhao, Y.; Jia, X. *ACS Appl. Mater. Interfaces* **2017**, *9*, 8910-8918.

(8) (a) Huang, R.; Wang, C.; Wang, Y.; Zhang, H. *Adv. Mater.* **2018**, *30*, 1800814; (b) Liu, H.; Lu, Z.; Zhang, Z.; Wang, Y.; Zhang, H. *Angew. Chem. Int. Ed.* **2018**, *57*, 8448-8452.

(9) Chandrasekar, R. *Phys. Chem. Chem. Phys.* **2014**, *16*, 7173-7183.

(10) Torres-Moya, I.; Martín, R.; Díaz-Ortiz, Á.; Prieto, P.; Carillo, J. R. *Isr. J. Chem.* **2018**, *58*, doi: ijch.201800030.

(11) Xiao, J.; Yin, Z.; Yang, B.; Liu, Y.; Ji, L.; Guo, J.; Huang, L.; Liu, X.; Yan, Q.; Zhang, H.; Zhang, Q. *Nanoscale* **2011**, *3*, 4720-4723:

(12) Saha, S; Desiraju, G. R. *J. Am. Chem. Soc.* **2017**, *139*, 1975-1983.

(13) Ahmed, E.; Karothu, D.P.; Naumov, P. *Angew. Chem. Int. Ed.* **2018**, *57*, 8837-8846.

(14) Turner, M. J.; Thomas, S.P.; Shi, M.W.; Jayatilaka, D.; Spackman, M. A. *Chem. Commun.* **2015**, *51*, 3735-3738.

(15) Glöckhofer, F.; Kautny, P.; Fritz, P.; Stöger, B.; Frölich, J. *ChemPhotoChem* **2017**, *1*, 51-55.

(16) (a) Würthner, F.; Kaiser, T. E.; Saha-Möller, C. R. *Angew. Chem. Int. Ed.* **2011**, *50*, 3376-3410: (b) Yoon, S.-J.: Chung, J. W.; Gierschner, J.; Kim, K. S.; Choi, M.-G.: Kim, D.; Park, S. Y. *J. Am. Chem. Soc*. **2010**, *132*, 13675-13683.

(17) Nicolini, T.; Famulari, A.; Gatti, T.; Marti-Rujas, J.; Villafiorita Monteleone F.; Canesi, E.V.; Meinardi, F.; Botta, C.; Parisini, E.; Meille, S. V.; Bertarelli *J. Phys. Chem. Lett.* **2014**, *5*, 2171-2176.

(18) We note that the related literature occasionally contains confusing terminology used to refer to the optical loss coefficient α (mm^{-1}) and α' (dB mm^{-1}). The values reported in the present article were corrected according to the explanation and the equations section 4 of the SI.

Table of Contents artwork